In Situ Control of Co-Continuous Phase Morphology for PS/PS-co-TMI/PA6 Blend

Cai-Liang Zhang, Tao Zhang, Lian-Fang Feng

State Key Laboratory of Chemical Engineering, Department of Chemical and Biological Engineering, Zhejiang University, 310027 Hangzhou, People's Republic of China
Correspondence to: L. F. FENG (E-mail: fenglf@zju.edu.cn)

ABSTRACT: The emulsification efficiency of PS-co-TMI, a copolymer polymerized by styrene and 3-isopropenyl-α,α-dimethylbenzene isocyanate (TMI), for polystyrene (PS)/polyamide 6 (PA6) blend was studied. During the mixing process, an effective emulsifier PS-g-PA6 was generated, which was demonstrated by differential scanning calorimetry (DSC) and fourier transform infrared spectroscopy. PS-g-PA6 generated by PS-co-TMI with high TMI content was found to contain some unreacted isocyanate active groups which reduced using efficiency of PS-co-TMI. Irrespective of TMI content in PS-co-TMI, the dosage of PS-co-TMI reached 20 wt %, unreacted PS-co-TMI was detected. These results indicated that reactive emulsification limits for both active groups' content and reactive precursors' dosage. After the rational addition of PS-co-TMI into PS/PA6 system, phase sizes of co-continuous structure were reduced conspicuously. However, co-continuous structure was evolved into matrix-dispersed structure while the dosage of PS-co-TMI reached 20 wt %. Emulsification efficiencies of PS-co-TMI with different TMI contents, 2.2, 4.1, and 7.5 wt %, were compared. The results revealed PS-co-TMI with 2.2 wt % TMI content had the highest reactive emulsification efficiency because of the block-copolymer-inclined emulsifier generated in the mixing process. © 2013 Wiley Periodicals, Inc. J. Appl. Polym. Sci. **2014**, *131*, 39972.

INTRODUCTION

Polymer materials with synergistic combination of desired properties can be achieved by blending existing polymers having different properties. Therefore, polymer blending has become a process of great importance for preparing high-performance polymeric materials. However, factors that affect the properties of the blends not only include the inherent properties of each polymer component, but also relate to the morphology of the blends. For a two-phase polymer blend, two types of morphologies can be encountered: matrix-dispersed phase and co-continuous phase. The latter is a three-dimensional interpenetrated structure, namely, both phases of the blend form the continuous phases. The blends with a co-continuous phase may find applications in conductive polymer field and strengthening polymer properties.[1–3] Therefore, much attention has been paid to this type of morphology.[4–9] For example, our previous work[3] reported that a pre-made graft copolymer can stop completely the coarsening of the co-continuous morphology under the quiescent annealing. Moreover, it was concluded that for graft copolymers with similar backbone and graft chain number, the longer the grafts, the higher their stabilizing efficiency; for a given backbone/graft composition, graft copolymers having

fewer and longer grafts were more efficient at compatibilizing and stabilizing the co-continuous morphology. However, this method adding directly premade copolymer has not been seen commercial success because the premade copolymer is difficult to obtain by industrial synthesis.

Reactive polymer blending has been considered as the most efficient way to stabilize the immiscible polymer blends in which polymer blending and chemical reactions take place simultaneously. It is an efficient process that integrates both the synthesis of emulsifier and polymer blending.[10,11] It would be interesting to generate co-continuous morphologies by reactive polymer blending. This work aimed at studying the co-continuous morphology development in a reactive polymer blending process. Polystyrene (PS) and polyamide 6 (PA6) was chosen as the blend system because incorporation of various functional groups, can react with amine and/or carboxylic acid end groups of PA6, to PS is relatively easy. In this work, the copolymer of styrene (St) and 3-isopropenyl-α, α-dimethylbenzene isocyanate (TMI), PS-co-TMI, was used as a reactive emulsifier precursor for the PS/PA6 blend. The effect of the TMI content in PS-co-TMI on the emulsification efficiency and the rule of co-continuous morphology development were

Table I. Selected Characteristics of PS and PA6 Used in This Work

	Number average molar mass[a] (M_n, kg/mol)	Mass average molar mass[a] (M_w, kg/mol)	Supplier
PS	101.3	228.8	Yangzi-BASF Styrenics, Nanjing, China
PA6	19.4	49.4	UBE Nylon, Thailand

[a] Molar mass measured by size exclusion chromatography (SEC) using PS standard for the calibration and tetrahydrofuran (THF) as the eluent. PA6 was first N-trifluoroacetylated prior to the SEC measurement.

investigated so as to further probe into the action principle of *in situ* emulsification technology.

EXPERIMENTAL

Materials

Two monomers used for synthesizing PS-co-TMI, St, and TMI, were purchased from Aldrich. The formula mass and the boiling temperature of TMI are 201 g/mol and 270°C/760 mmHg, respectively. Prior to the co-polymerization, St was purified over an aluminum oxide column and TMI was not subjected to any purification. Benzoyl peroxide (BPO) was used as the free radical initiator. It was purified by dissolution in methanol, precipitation in chloroform and then was dried in a vacuum oven at room temperature. Toluene was used as the solvent for copolymerization and was purified by boiling in the presence of anhydrous calcium oxide. Formic acid was purchased from Yixing Second Chemical Reagent Factory of China. Table I shows selected characteristics of PS and PA6 used in this work.

Synthesis of PS-co-TMI

PS-co-TMI was prepared by solution polymerization using a 2-L glass reactor equipped with a mechanical agitator. The synthesis processes were as follows: toluene was first charged to the reactor followed by St, TMI, and BPO. The reactor was purged by nitrogen and the temperature was controlled at 80°C by oil bath. The polymerization process lasted for 24 hours. The obtained product was precipitated twice in the methanol, filtered, and then dried in the vacuum oven at 80°C for 24 hours.[12–16] PS-co-TMI with different TMI contents were obtained upon varying the proportion of St and TMI in the synthesis process.[15,16]

Polymer Blending Process

A Brabender torque rheometer, which has a volume capacity of 50 mL and is equipped with two screws, was used for preparing PS/PS-co-TMI/PA6 blends. In the blending process, the two screws rotated in an opposite direction to ensure good mixing. Prior to the blending, PS, PS-co-TMI, and PA6 were dried in a vacuum oven at 80°C for 12 hours. For the blend systems, the mass ratio between PS and PA6 was always unity, and the concentrations of PS-co-TMI in the blends were 10, 15, and 20 wt %. The dried components were charged simultaneously into the mixing chamber and were mixed with a rate of 100 revolutions per minute (rpm) at 230°C. After 10 min of mixing, samples were quickly taken from the chamber and then were quenched in the liquid nitrogen to freeze-in their morphologies.

Fourier Transform Infrared Spectroscopy Analysis

Solid samples were pressed into films of 40–90 μm thick under 230°C and 30 MPa for 1 min. For solution samples, films were made after dipping solutions into the potassium bromide (KBr) flake and then dried under infrared light. Fourier transform infrared spectroscopy (FTIR) tests were performed on Nicolet 5700 with a scanning speed of 32 s^{-1} and a resolution of 4 cm^{-1}.

Differential Scanning Calorimetry Measurement

The melting and crystallization behavior of PA6 and melting behavior of PS were studied using a differential scanning calorimetry (DSC) of type DSC7 from PerkinElmer under the nitrogen atmosphere. Samples were subjected to the following thermal cycle: all samples were heated from 50°C to 260°C at a rate of 10°C/min and the temperature was maintained at 260°C for 2 min in order to erase previous thermal histories. Then, they were cooled down to 50°C at a rate of 10°C/min to follow their crystallization behavior. Finally, they were heated back to 260°C at a rate of 10°C/min to follow their melting behavior.

Scanning Electron Microscopy Characterization

Morphologies of polymer blends were analyzed by scanning electron microscopy (SEM). Samples were quenched in the liquid nitrogen to facilitate their fracture. The fractured samples were later immersed in formic acid for 12 hours to remove PA6 domains in each blend. They were dried in a vacuum oven at 80°C for 12 hours. The etched surfaces were gold-sputtered for subsequent SEM analysis on Philips SIRON-100 SEM.

SEC Measurement

Polyamide is insoluble in classical organic solvents such as tetrahydrofuran (THF) at room temperature. However, it becomes soluble in such solvents after it is subjected to the reaction with trifluoroacetic anhydride (TFAA) which leads to N-trifluoroacetylated derivatives (PA-TFAA).[17] PA-TFAA can then be characterized by SEC using THF as the eluent and PS standard for the calibration.[18,19] PS-co-TMI was directly soluble in THF for SEC measurement.

RESULTS AND DISCUSSION

Characteristic of PS-co-TMI

Figure 1 shows the FTIR spectra of three PS-co-TMI samples containing various TMI contents. They are characterized by a peak at 2255 cm^{-1} corresponding to the isocyanate group of the TMI and by another one at 1492 cm^{-1} corresponding to St. The latter peak was chosen as the internal reference and the former peak was used to determine TMI content in PS-co-TMI. Based on the relationship between TMI content and the peak absorbency ratio between the peak at 2255 cm^{-1} and that at 2772 cm^{-1} established in an early work,[20] the TMI content was 2.2, 4.1, and 7.5 wt % for PS-co-TMI2, PS-co-TMI4, and PS-co-TMI8, respectively. Table II gathers information about initial compositions of the copolymerization system, TMI contents, and molar masses of the resulting PS-co-TMI.
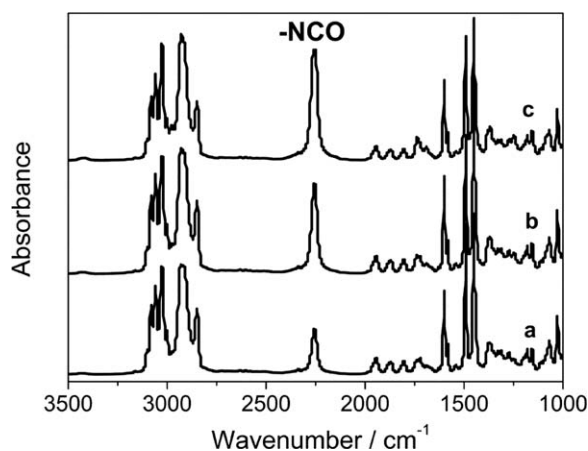
Figure 1. FTIR spectra of PS-co-TMI containing various amounts of TMI: (a) PS-co-TMI2; (b) PS-co-TMI4; and (c) PS-co-TMI8.

Characteristics of the PS-g-PA6 Copolymers

The isocyanate group of the PS-co-TMI may be able to react with the terminal amine group of PA6, leading to the formation of a PS-g-PA6 graft copolymer, as shown in Figure 2. In order to isolate the pure PS-g-PA6 graft copolymer from the PS/PS-co-TMI/PA6 blend, the latter was first pressed into a film of about 1 mm thickness at 230°C and then was subjected to dissolution THF at room temperature for 7 days to ensure complete removal of the PS phase. What was not dissolved in THF was immersed in formic acid for 12 hours in order to fully dissolve the PA6 phase. The resulting material which was not soluble in THF or formic acid was supposed to be the pure PS-g-PA6 graft copolymer.

Figure 3 shows the DSC thermograms of the pure PS-g-PA6 graft copolymer formed in the PS/PS-co-TMI8/PA6 (40/20/40 by mass) blend system. In the heating cycle, a small peak rises around 110°C, corresponding to the glass transition temperature of the PS. There are two peaks at 210°C and 220°C, corresponding to α-PA6 and γ-PA6, respectively.[21] In the cooling cycle, there is a peak at 185°C, corresponding to the crystallization of the PA6 grafts.

Figure 4 shows the FTIR spectra of the above pure PS-g-PA6 graft copolymer. The peaks at around 3300 and 1492 cm^{-1} are characteristic ones of N-H moieties from PA6 grafts and the benzene ring from PS backbone, respectively.

Semi-Quantitative Characterization of the Interfacial Reaction Between PS-co-TMI and PA6

The amount of the isocyanate moieties in the PS/PS-co-TMI/PA6 composition before and after blending is a rough measurement of the degree of the interfacial reaction between PS-co-TMI and PA6 or the amount of the PS-g-PA6 graft copolymer formed. There are two types of isocyanate moieties after blending: the one in PS-co-TMI chains that has partly reacted with the terminal amine group of the PA6 and the other one in PS-co-TMI chains that remain intact during the blending process.

To determine those two different types of the isocyanate moieties in the blend, it was necessary to isolate the various types of components. However, formic acid could not be used because it was not only capable of dissolving PA6 but also reacting with the isocyanate moieties of PS-co-TMI. Figure 5 shows the comparison between spectra of PS-co-TMI4 before and after immersion in formic acid for 2 days. After the formic acid treatment, the characteristic peak of isocyanate moieties at 2250 cm^{-1} has almost completely disappeared, indicating that formic acid can react with the isocyanate moieties, as we expected.

In order to determine those two types of isocyanate moieties in PS/PS-co-TMI/PA6 blends, all blends were immersed in THF at room temperature for 7 days. Two fractions were then obtained. The one soluble in THF was supposed to be the PS and the PS-co-TMI that remained intact during the blending process and the one insoluble in THF was believed to be the PA6 and PS-g-PA6 graft copolymer. The PS backbone of the PS-g-PA6 graft copolymer could contain isocyanate moieties.

Figures 6–8 show the FTIR spectra of the fraction soluble in THF. There is a peak at 2250 cm^{-1} characteristic of the isocyanate moiety for the PS/PS-co-TMI/PA6 blends containing 20 wt % PS-co-TMI. This indicates that part of the PS-co-TMI chains remain completely intact during the entire polymer blending process. That peak is very small or inexistent when the PS-co-

Table II. Initial Compositions for the Synthesis, and TMI Contents and Molar Mass of the Resulting PS-co-TMI

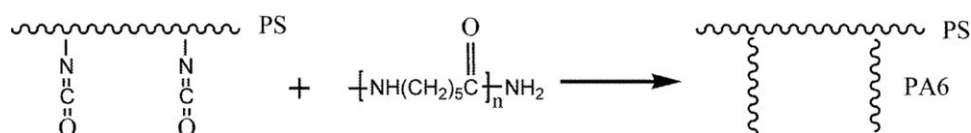| Samples	Toluene/St/TMI/BPO	TMI content (wt %)	Molar number of isocyanate per PS-co-TMI (mol/g)	M_n (kg/mol)
PS-co-TMI2	60 mL/40 mL/0.8 mL/0.2 g	2.2	1.1×10^{-4}	31.4
PS-co-TMI4	60 mL/40 mL/1.6 mL/0.2 g	4.1	2.0×10^{-4}	37.1
PS-co-TMI8	60 mL/40 mL/3.2 mL/0.2 g	7.5	3.7×10^{-4}	39.8

Figure 2. Mechanism of the formation of PS-g-PA6 graft copolymer by interfacial reaction between isocyanate group of the PS-co-TMI and the terminal amine group of PA6.
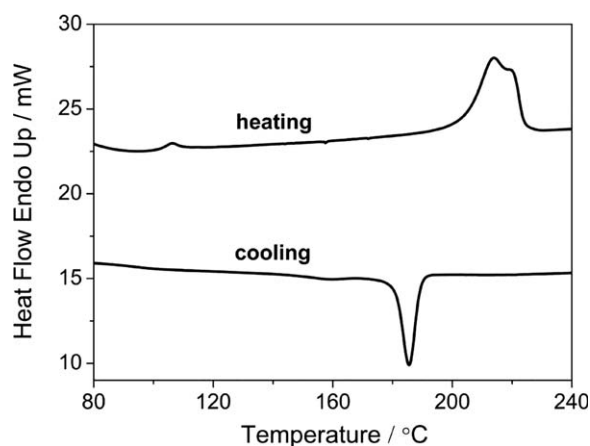
Figure 3. DSC thermograms of a pure PS-g-PA6 graft copolymer formed in PS/PS-co-TMI8/PA6 (40/20/40 by mass).

TMI contents were below 15 wt %, implying that most of the PS-co-TMI chains, if not all, had participated in the interfacial reaction. An excess of PS-co-TMI was therefore useless for emulsification.
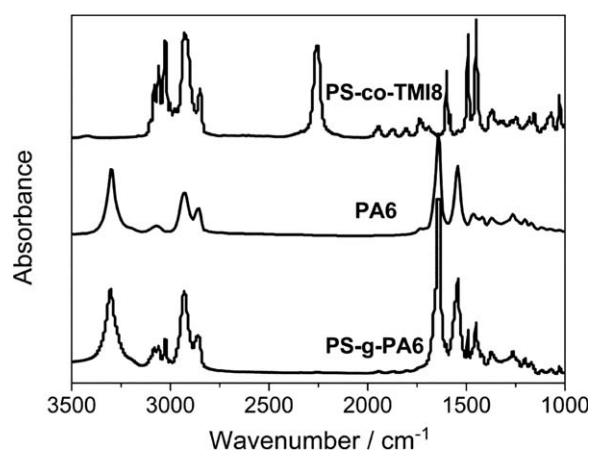

Figure 4. FTIR spectra of PS-co-TMI8, PA6, and the pure PS-g-PA6 graft copolymer obtained from the PS/PS-co-TMI8/PA6 (40/20/40 by mass) blend.
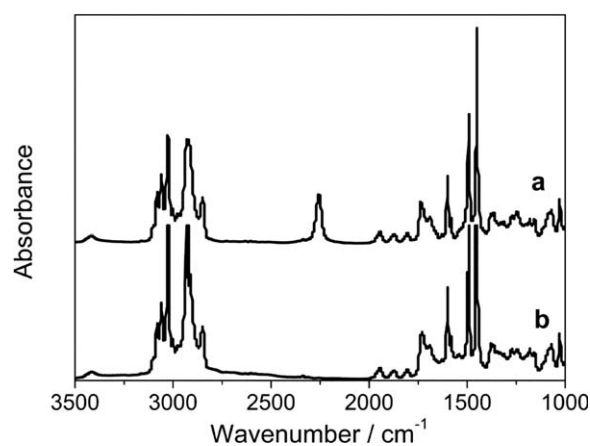

Figure 5. FTIR spectra of PS-co-TMI4 before and after immersion in formic acid: (a) before immersion; and (b) after immersion.
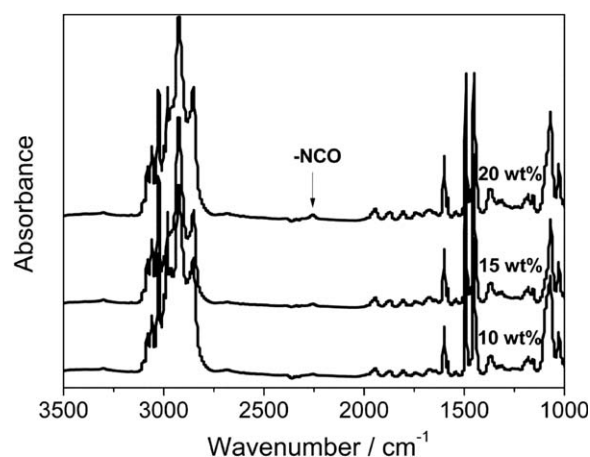

Figure 6. FTIR spectra of the fraction soluble in THF for the PS/PA6 (1/1 by mass) blends with PS-co-TMI2 as the compatibilizer. PS-co-TMI2 dosage is 10, 15, and 20 wt %, respectively.
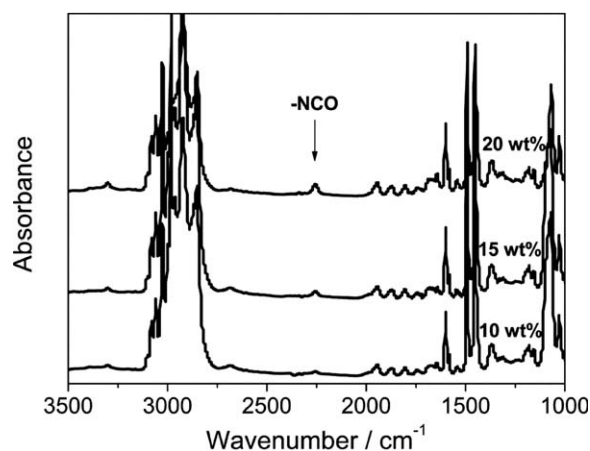

Figure 7. FTIR spectra of the fraction soluble in THF for the PS/PA6 (1/1 by mass) blends with PS-co-TMI4 as the compatibilizer. PS-co-TMI4 dosage is 10, 15, and 20 wt %, respectively.
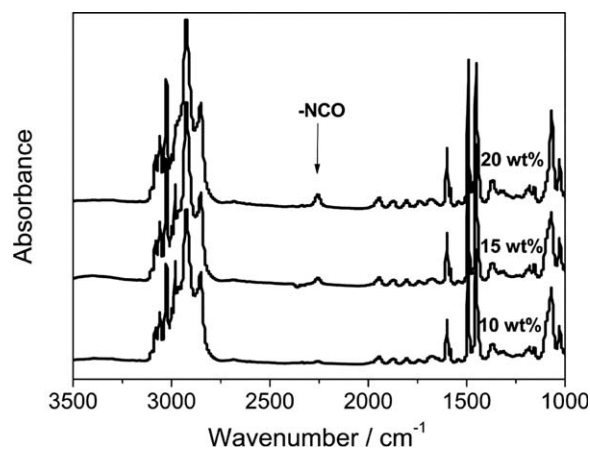

Figure 8. FTIR spectra of the fraction soluble in THF for the PS/PA6 (1/1 by mass) blends with PS-co-TMI8 as the compatibilizer. PS-co-TMI8 dosage is 10, 15, and 20 wt %, respectively.
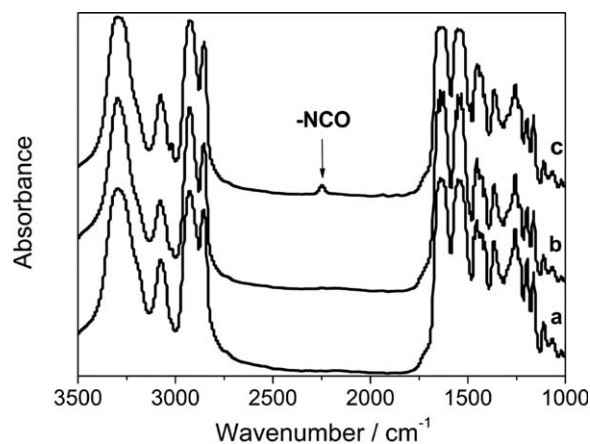
Figure 9. FTIR spectra of the fraction insoluble in THF for the PS/PS-co-TMI/PA6 (40/20/40 by mass) blends: (a) PS-co-TMI2, (b) PS-co-TMI4, and (c) PS-co-TMI8.

Figure 10. FTIR spectra of the fraction insoluble in THF for the PS/PS-co-TMI8/PA6 blends: (a) 45/10/45 by mass, (b) 42.5/15/42.5 by mass, and (c) 40/20/40 by mass.

Figure 9 compares the FTIR spectra of the fraction insoluble in THF for the PS/PS-co-TMI/PA6 (40/20/40 by mass) blends containing various PS-co-TMI with different TMI content. In the case of PS-co-TMI2 and PS-co-TMI4, the peak at 2250 cm^{-1} characteristic of the isocyanate moieties is almost undetectable, implying that all isocyanate moieties in them had reacted with the terminal group of the PA6 during the polymer blending process. In the case of PS-co-TMI8, the peak at 2250 cm^{-1} is detected, indicating that not all isocyanate moieties in the PS-co-TMI8 had reacted during the polymer blending process. Figure 10 shows that it is true even when the PS-co-TMI8 content is much lower. It could be one reason that the amount of isocyanate was still in large excess compared to the terminal amine group of PA6. As shown in Table II, the molar number of the isocyanate per gram of PS-co-TMI8 is 3.7×10^{-4}, which is five times higher than that of terminal amine group per gram of PA6 obtained by conductance titration. The other reason may result from steric hindrance of TMI thus lower the reactive efficiency of PS-co-TMI. In any event, the excess isocyanate of PS-co-TMI with high TMI content may be useless for emulsification.

Phase Morphologies

Figure 11 shows the SEM micrographs of PS/PA6 (50/50 by mass) and PS/PS-co-TMI4/PA6 blends containing various amounts of PS-co-TMI4. The morphology of the PS/PA6 (50/50 by mass) blend is co-continuous. It remains co-continuous with
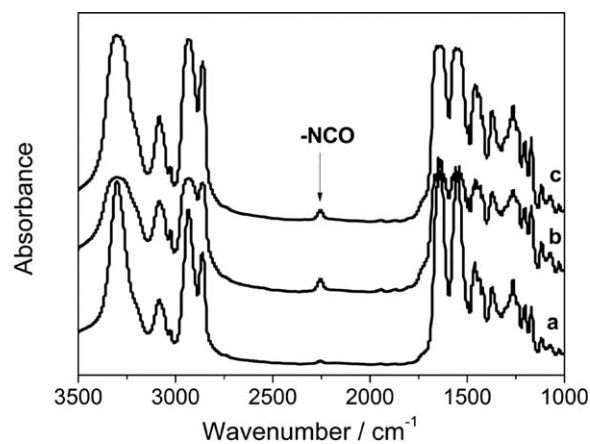
15 wt % PS-co-TMI4. Nevertheless, the phase size was significantly reduced. With 20 wt % PS-co-TMI4, the morphology is not co-continuous any more but of the sea-island structure. Our previous research[5] found that the morphology of the PS/PA6 blend evolved from a co-continuous morphology without an emulsifier to a sea-island structure with 1 wt % PS-g-PA6 graft copolymer. Zhao[22] found that adding a copolymer of St and maleic anhydride resulted in a narrower co-continuous composition for the PS/PA6 blend. The transition from a co-continuous morphology to a sea-island structure observed in this work could be related to the fact that the addition of PS-co-TMI resulted in the formation of the PS-g-PA6 graft copolymer. Consequently the mass ratio between PS/PA6 and concomitantly their volume ratio was further deviated from unity, favoring the evolution of the co-continuous morphology to the sea-island structure.

Figure 12 shows the effects of different amounts of TMI and PS-co-TMI on the morphology of the PS/PS-co-TMI/PA6 blend. Compared with the PS/PA6 (50/50 by mass) blend as shown in Figure 11(A), adding 1 wt % PS-co-TMI does not change much the co-continuous phase size. When the amount of PS-co-TMI is increased to 5 wt %, the phase size is much smaller. A further increase in the amount of PS-co-TMI leads to a further decrease in the phase size of co-continuous morphology. It is also seen that the TMI content in PS-co-TMI has a significant impact on the co-continuous morphology size. For a given amount of PS-co-TMI, its emulsification efficiency follows the order:
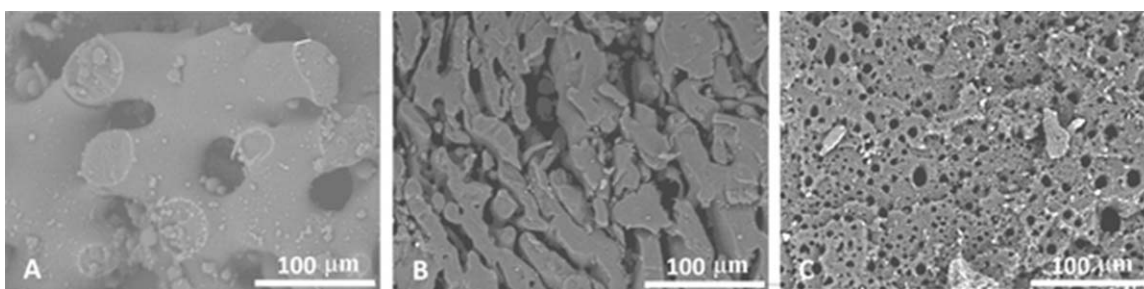

Figure 11. Effect of the PS-co-TMI4 content on the morphology of the PS/PS-co-TMI4/PA6 blend: (A) PS/PA6 (50/50 by mass); (B) PS/PS-co-TMI4/PA6 (42.5/15/42.5 by mass); and (C) PS/PS-co-TMI4/PA6 (40/20/40 by mass).
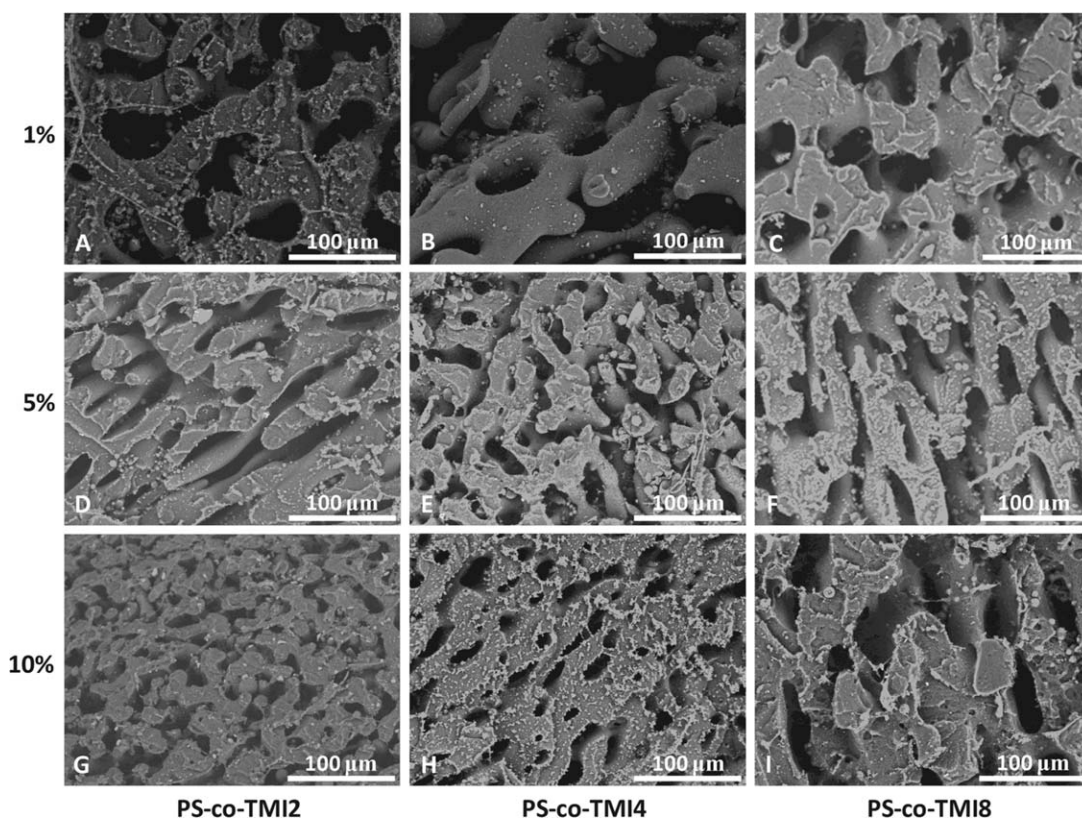
Figure 12. Morphology of polymer blending system under different TMI contents and different dosages of PS-co-TMI: (A) PS/PS-co-TMI2/PA6 (49.5/1/49.5 by mass); (B) PS/PS-co-TMI4/PA6 (49.5/1/49.5 by mass); (C) PS/PS-co-TMI8/PA6 (49.5/1/49.5 by mass); (D) PS/PS-co-TMI2/PA6 (47.5/5/47.5 by mass); (E) PS/PS-co-TMI4/PA6 (47.5/5/47.5 by mass); (F) PS/PS-co-TMI8/PA6 (47.5/5/47.5 by mass); (G) PS/PS-co-TMI2/PA6 (45/10/45 by mass); (H) PS/PS-co-TMI4/PA6 (45/10/45 by mass); and (I) PS/PS-co-TMI8/PA6 (45/10/45 by mass).

PS-co-TMI2 > PS-co-TMI4 > PS-co-TMI8. At first glance, this could be surprising because the TMI content in PS-co-TMI follows exactly the opposite order. When the TMI content in PS-co-TMI is very high, the number of isocyanate moieties per PS backbone is very high. As the reaction between PS-co-TMI and PA6 is occurring at the PS/PA6 interfaces, the number of PA6 grafts in the PS-g-PA6 graft copolymer may increase. When the latter reaches a certain critical threshold, the PS-g-PA6 may no longer stay at the PS/PA6 interfaces but migrate to the PA6 phase. Once it is in the PA6 phase, it does not have emulsification efficiency any more. Moreover, the remaining isocyanate moieties in the PS-g-PA6 graft copolymer may further react with PA6, consuming uselessly the PA6 chains. Therefore, PS-co-TMI with a very high TMI may be less efficient for compatibilizing PS/PA6 blends. Our previous results[23] showed that for *in situ* emulsification of polymer blend, reactive block copolymer as emulsifier precursor was more efficient than reactive graft copolymer. It may be concluded that the reactive graft copolymer such as PS-co-TMI with block-inclined-polymer structure have the highest emulsification efficiency.

CONCLUSIONS

This work deals with co-continuous morphology development in PS/PA6 reactive blend system. PS-co-TMI with different TMI contents were acted as the reactive precursors. In the polymer reactive mixing process, the effective emulsifier PS-g-PA6 was generated.

PS-g-PA6 produced by PS-co-TMI with high TMI content were found containing unreacted isocyanate active groups which may be caused by the steric effects of TMI groups; and the mixing system using high dosage of PS-co-TMI were found containing unreacted PS-co-TMI. All these results indicate that reactive emulsification limits for both dosage and active groups' content in PS-co-TMI. By increasing the dosage of PS-co-TMI, phase structure transformed from co-continuous morphology into matrix-dispersed structure, contributed by the emulsifying effect of generated PS-g-PA6 and volume ratio change between PS and PA6. The emulsification efficiencies of three different PS-co-TMI samples were also compared, PS-co-TMI-2 turned out to have the best emulsification efficiency, which may be because of its block-inclined-polymer structure.

REFERENCES

1. Willemse, R. C.; Speijer, A.; Langeraar, A. E.; Posthuma de Boer, A. *Polymer* **1999**, *40*, 6645.

2. Niebergall, U. Ph.D. Thesis, TU Berlin, Berlin, **1998**.

3. Niebergall, U.; Bohse, J.; Seidler, S.; Grellmann, W.; Schürmann, B.L. *Polym. Eng. Sci.* **1999**, *39*, 1109.

4. Pu, G. W.; Luo, Y. W.; Lou, Q.; Li, B. *Macromol. Rapid Commun.* **2009**, *30*, 133.

5. Zhang, C. L.; Feng, L. F.; Zhao, J.; Huang, H.; Hoppe, S.; Hu, G. H. *Polymer* **2008**, *49*, 3462.

6. Lopez-Barron, C. R.; Macosko, C. W. *J. Rheology* **2012**, *56*, 1315.

7. Trifkovic, M.; Hedegaard, A.; Huston, K.; Sheikhzadeh, M.; Macosko, C. W. *Macromolecules* **2012**, *45*, 6036.

8. Bell, J. R.; Chang, K.; Lopez-Barron, C. R.; Macosko, C. W.; Morse, D. C. *Macromolecules* **2010**, *43*, 5024.

9. Daux, V.; Prochazka, F.; Carrot, C. *J. Appl. Polym. Sci.* **2013**, *128*, 265.

10. Tsou, A. H.; Favis, B. D.; Hara, Y.; Bhadane, P. A.; Kirino, Y. *Macromol. Chem. Phys.* **2009**, *210*, 340.

11. Shashidhara, G. M.; Biswas, D.; Pai, B. S.; Kadiyala, A. K.; Feroze, G. S. W.; Ganesh, M. *Polym. Bull.* **2009**, *63*, 147.

12. Mohammed, S.; Daniels, E. S.; Klein, A.; El-Aasser, M. S. *J. Appl. Polym. Sci.* **1998**, *67*, 559.

13. Wu, H. S.; Chuang, M. H.; Hwang, J. W. *J. Appl. Polym. Sci.* **1999**, *73*, 2763.

14. Leonie, B.; Christopher, B. K.; Thomas, P. D. *J. Polym. Sci. Part A: Polym. Chem.* **2002**, *40*, 1064.

15. Zhang, C. L.; Feng, L. F.; Hoppe, S.; Hu, G. H. *J. Polym. Sci. Part A: Polym. Chem.* **2008**, *46*, 4766.

16. Zhang, C. L.; Feng, L. F.; Gu, X. P.; Hoppe, S. Hu, *G. H. Polym. Eng. Sci.* **2011**, *51*, 2261.

17. Schuttenberg, H.; Schulz, R. C. *Angew. Chem. Int. Ed.* **1976**, *15*, 777.

18. Weisskopf, K. *Polymer* **1985**, *26*, 1187.

19. Zhang, C. L.; Feng, L. F.; Gu, X. P.; Hoppe, S.; Hu, G. H. *Polym. Test.* **2007**, *26*, 793.

20. Li, G. Z.; Feng, L. F.; Gu, X. P.; Xu, Z. B.; Hu, G. H. *J. Funct. Polym.* **2005**, *18*, 127.

21. Pötschke, P.; Paul, D. R. *Macromol. Symp.* **2003**, *198*, 69.

22. Zhao, J.; Xu, Z. B.; Feng, L. F. *J. Mater. Eng.* **2006**, *8*, 36.

23. Yu, Q. Y.; Zhang, C. L.; Gu, X. P.; Wang, J. J.; Feng, L. F. *J. Appl. Polym. Sci.* **2012**, *124*, 3392.